



Article

Remote Sensing Extraction of Lakes on the Tibetan Plateau Based on the Google Earth Engine and Deep Learning

Yunxuan Pang^{1,2,3}, Junchuan Yu^{2,3,*} , Laidian Xi^{1,2,3}, Daqing Ge^{2,3}, Ping Zhou¹ , Changhong Hou^{2,3,4}, Peng He^{2,3} and Liu Zhao⁵

- ¹ School of Earth Sciences and Resources, China University of Geosciences (Beijing), Beijing 100083, China; 2101210161@email.cugb.edu.cn (Y.P.); 2101210160@email.cugb.edu.cn (L.X.); zhoupx@cugb.edu.cn (P.Z.)
 - ² Department of Research and Development, China Aero Geophysical Survey and Remote Sensing Center for Natural Resources, Beijing 100083, China; gedaqing@mail.cgs.gov.cn (D.G.); bqt2300203041@student.cumtb.edu.cn (C.H.); hepeng@mail.cgs.gov.cn (P.H.)
 - ³ Technology Innovation Center for Geohazard Identification and Monitoring with Earth Observation System, MNR, Beijing 100083, China
 - ⁴ School of Geosciences and Surveying Engineering, China University of Mining and Technology (Beijing), Beijing 100083, China
 - ⁵ School of Geography, Planning and Spatial Sciences, University of Tasmania, Hobart, TAS 7005, Australia; lzhaol1@utas.edu.au
- * Correspondence: yujunchuan@mail.cgs.gov.cn; Tel.: +86-151-0115-7141

Abstract: Lakes are an important component of global water resources. In order to achieve accurate lake extractions on a large scale, this study takes the Tibetan Plateau as the study area and proposes an Automated Lake Extraction Workflow (ALEW) based on the Google Earth Engine (GEE) and deep learning in response to the problems of a low lake identification accuracy and low efficiency in complex situations. It involves pre-processing massive images and creating a database of examples of lake extraction on the Tibetan Plateau. A lightweight convolutional neural network named LiteConvNet is constructed that makes it possible to obtain spatial-spectral features for accurate extractions while using less computational resources. We execute model training and online predictions using the Google Cloud platform, which leads to the rapid extraction of lakes over the whole Tibetan Plateau. We assess LiteConvNet, along with thresholding, traditional machine learning, and various open-source classification products, through both visual interpretation and quantitative analysis. The results demonstrate that the LiteConvNet model may greatly enhance the precision of lake extraction in intricate settings, achieving an overall accuracy of 97.44%. The method presented in this paper demonstrates promising capabilities in extracting lake information on a large scale, offering practical benefits for the remote sensing monitoring and management of water resources in cloudy and climate-differentiated regions.

Keywords: Google Earth Engine; deep learning; Tibetan Plateau; lake; cloud computing



Citation: Pang, Y.; Yu, J.; Xi, L.; Ge, D.; Zhou, P.; Hou, C.; He, P.; Zhao, L. Remote Sensing Extraction of Lakes on the Tibetan Plateau Based on the Google Earth Engine and Deep Learning. *Remote Sens.* **2024**, *16*, 583. <https://doi.org/10.3390/rs16030583>

Academic Editors: Armin Moghimi, Meisam Amani, Mohammad Kakooei, Reza Shah-Hosseini, Masood Varshosaz and Ali Mohammadzadeh

Received: 26 December 2023

Revised: 31 January 2024

Accepted: 31 January 2024

Published: 3 February 2024



Copyright: © 2024 by the authors. Licensee MDPI, Basel, Switzerland. This article is an open access article distributed under the terms and conditions of the Creative Commons Attribution (CC BY) license (<https://creativecommons.org/licenses/by/4.0/>).

1. Introduction

As an important water resource, lakes are not only important information carriers that reveal changes in the climate [1], environment [2], and hydrology [3], but also important natural resources for human survival and development, and they play a vital role in maintaining species, the environment, and ecological security [4].

Remote sensing is a critical method for obtaining lake-related information, and its application began in 1974 [5]. With the rapid advancement of remote sensing [6], threshold methods based on water indices have been introduced, such as the normalized difference water index (NDWI) [7] and modified normalized difference water body index (MNDWI) [8]. Wang et al. [9] compared the accuracy of different indices for extracting lake boundaries based on Landsat 8 OLI images with Dianchi Lake, Fuxian Lake, Yangzonghai

Lake, Xingyun Lake, and Qicai Lake as samples. The MNDWI index, obtained through analysis, proves to be more precise in extracting the water boundary of eutrophic lakes. Deoli et al. [10] discerned diffusion area trends for Nainital Lake based on calculated NDWI values, a study that aids governmental and policymaker decision making in crafting reclamation and restoration plans for Nainital Lake. Thresholding is a straightforward, intuitive, easily implemented, and computationally efficient method. However, image classification based on preset thresholds unavoidably requires human intervention and adjustment. To address this issue, the Otsu method was introduced for lake extraction. The Otsu method partially solves the problems associated with threshold segmentation by adjusting the threshold to adaptively distinguish water from the background. Tran et al. [11] employed a dynamic Otsu threshold based on Sentinel-1 images to ascertain the optimal threshold for segmentation in the Mekong Delta region. This enabled the extraction of water and the creation of time-series maps for the extensive mapping of surface water and monitoring of floods. The use of the dynamic Otsu threshold algorithm involves scanning entire images, which can result in a significant computational burden. Therefore, it may not always be suitable for large-scale applications.

With the development of computer technology, traditional machine learning methods are gradually becoming a better choice for water body extraction. Sarp et al. [12] employed support vector machine classification and spectral water indices, demonstrating a substantial reduction in the surface area of water in Lake Bourdur between 1987 and 2011. Nhu et al. [13] applied machine learning techniques, including random forests and M5P, to investigate Lake Zrebar, one of Iran's largest freshwater lakes, and also forecasted daily water levels. Traditional machine learning methods overcome the problem of manual threshold setting through the learning process; however, since these methods use the pixel as a computational unit, the spatial information is not fully in use, resulting in a "salt and pepper" effect in the results. The advent of deep learning technology introduces innovative solutions for lake extraction. Convolutional neural networks, with their powerful feature extraction capabilities, are able to make better use of the spatial-spectral information of the image, which helps to improve the differentiation of targets such as water bodies, shadows, and glaciers. Yu et al. [14] developed a convolutional neural network-based method for delineating water bodies from Landsat images by taking into account information pertaining to both spectral and spatial characteristics. Wang et al. [15] presented an end-to-end trainable model named MSLWENet to improve the extraction results of small lakes. This model specifically tackles the challenge of large intra-class variance and small inter-class variance when it comes to lakes' water bodies.

Improvements in lake extraction methods have not solved all the problems in large-scale applications. How to quickly process and analyze images is a serious issue facing the age of big data [16]. The development of high-performance cloud computing platforms has provided new technical support. The Google Earth Engine (GEE) is a comprehensive platform for remote sensing, science analysis, and the visualization of geospatial data [17]. The GEE has an extensive range of remote sensing resources that enable researchers to synchronize with multiple remote sensor data sources and quickly process data online to provide solutions for wide-ranging applications [18], such as global forest changes [19], natural hazard assessments [20], land use/land cover mappings [21], urban studies [22], disease risk assessments [23], and crop classifications [24]. Furthermore, the GEE offers deep learning techniques, which are essential for enhancing the overall performance of applications and are particularly important for processing remote sensing images and analyzing data. Wang et al. [25] used remote sensing data-based indices and pixel-level water detection algorithms on the GEE platform to calculate the flooding frequency. Sha et al. [26] combined NDWI, MNDWI, and SVM methods to extract Tosu Lake. Wang et al. [27] developed an Automatic Water Extraction Model in Complex Environments based on the GEE to extract water in intricate surroundings. Chen et al. [28] generated a glacial lake map of the TP region for 2015 based on the non-local active contour algorithm and Landsat 8 images. Zhang et al. [29] developed a per-pixel composited method named

the “multitemporal mean NDWI composite” to automatically extract the glacial lake area. Recently, some scholars have combined deep learning with the GEE, which provides a new solution for water extraction in large-scale regions, and progress has been made in model design, deployment, and the automated creation of samples [30–32]. However, further research in these areas remains to be explored.

At present, there are relatively few studies on lake extraction on a large regional scale, and the research related to the combination of the GEE and deep learning needs to be further deepened. And there are a large number of parameters available for deep learning models for lake extraction, which makes it difficult to meet the need for real-time prediction. How to construct a lightweight convolutional neural network (CNN) to ensure inference efficiency under the premise of obtaining a better lake extraction is the current problem. Therefore, this study combined deep learning and the GEE to identify lake information based on a wide range of high-altitude areas. The objectives of this study were as follows: (1) Propose an Automated Lake Extraction Workflow (ALEW) that integrates a deep learning model and develops a lightweight CNN called LiteConvNet, specifically designed to handle the complex conditions seen on the Tibetan Plateau; (2) Create a lake extraction dataset on the Tibetan Plateau for LiteConvNet model training using the GEE platform; and (3) Explore the LiteConvNet model within the ALEW process for the purpose of identifying lakes.

2. Materials and Methods

2.1. Study Area

The Tibetan Plateau in China is situated centrally within the Asian continent, at an average altitude of more than 4000 m. It spans a total area of over 2.5 million square kilometers, which is 26.8 percent of the country’s entire geographical area [33]. It mainly covers the entire province of Qinghai and the Tibetan Autonomous Region, as well as the southwestern regions of Gansu Province, the northern region of Sichuan, northwestern Yunnan, and the southern areas of the Xinjiang Uighur autonomous region [34,35]. The geographic location of the Tibetan Plateau is shown in Figure 1. The Tibetan Plateau, referred to as the Earth’s third pole and the Asian water tower, possesses distinctive climatic and geographical characteristics that support an intricate and varied ecology. It serves as a crucial ecological security barrier in China and the wider Asian region.

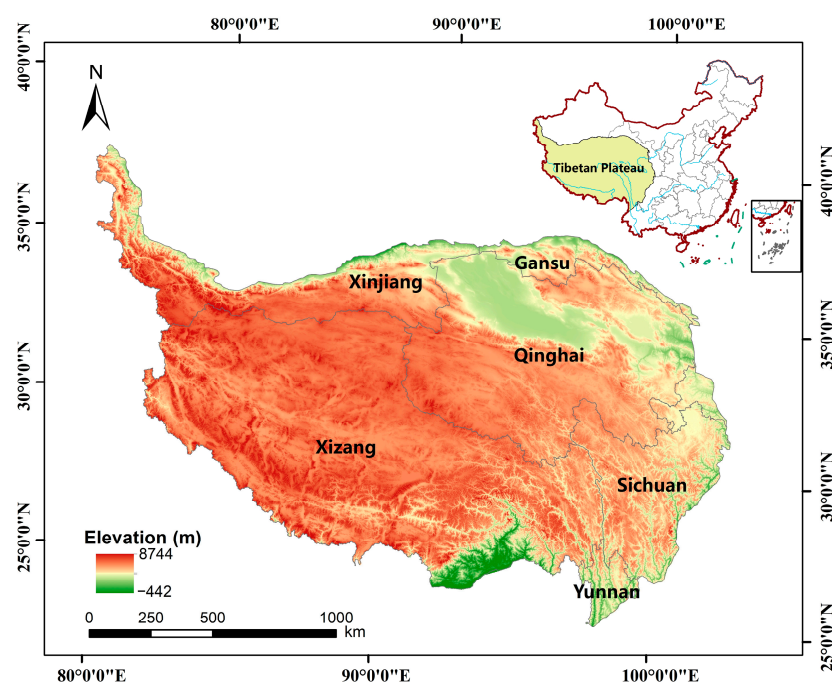


Figure 1. The geographic location of the Tibetan Plateau.

2.2. Data Sources

The Sentinel-2 Level-2A images available on the GEE platform were used for this study. The data underwent radiometric calibration, atmospheric correction, and orthorectification [36]. The Copernicus Programme of the European Space Agency encompassed the deployment of Sentinel-2, a satellite equipped with advanced multispectral imaging capabilities and capable of capturing high-resolution imagery. The Multispectral Imager (MSI) is an advancement and continuation of both the US Land Satellite and China's High-Resolution Satellite programs [37]. The Sentinel-2 constellation revisits the same location every 5 days and has a spatial resolution of 10 m. The Sentinel-2 constellation has a shorter revisit duration and a higher spatial resolution, making it a more suitable option for large-scale remote sensing classification applications [38].

In our study, June to October 2021 was selected as the study period because of the plentiful water supply of lakes in the Tibetan Plateau during the abundant season. We directly accessed the Sentinel-2A images by writing code online on the GEE platform. We filtered 4977 images within the study area based on the acquisition date and a cloud cover of less than 20%. The image coverage of the study area is shown in Figure 2. As the QA60 band of Sentinel-2A contains the cloud mask information, we used it for cloud removal. The next step was to mosaic all the images. Finally, the image was clipped according to the vector boundary of the Tibetan Plateau that we uploaded to obtain the high-quality image.

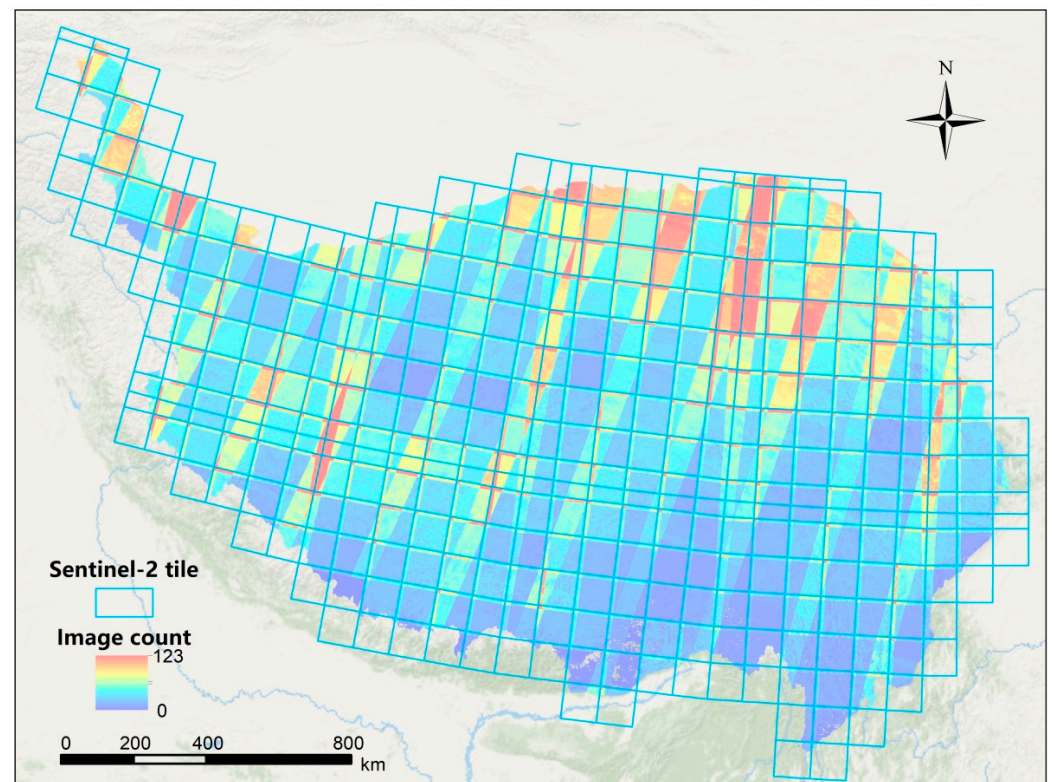


Figure 2. The coverage of Sentinel-2 images in the study area.

2.3. Methodology

To enable the real-time extraction of lakes on the Tibetan Plateau through deep learning technology, we propose a process termed ALEW (Automated Lake Extraction Workflow) designed for implementation on the GEE cloud platform. The entire procedure comprises three primary components. First, the GEE cloud platform is employed to perform pre-processing tasks such as Sentinel-2 data screening and cloud removal. Secondly, the generation of a training sample dataset is achieved through automated sample collection and slicing. Thirdly, a lightweight CNN model is constructed and trained using the Google

Colab platform. On the GEE platform, we employed trained models to make real-time inferences on lakes situated across the Tibetan Plateau. Finally, the results were compared to different algorithms and open-source water products. The overall workflow diagram is shown in Figure 3.

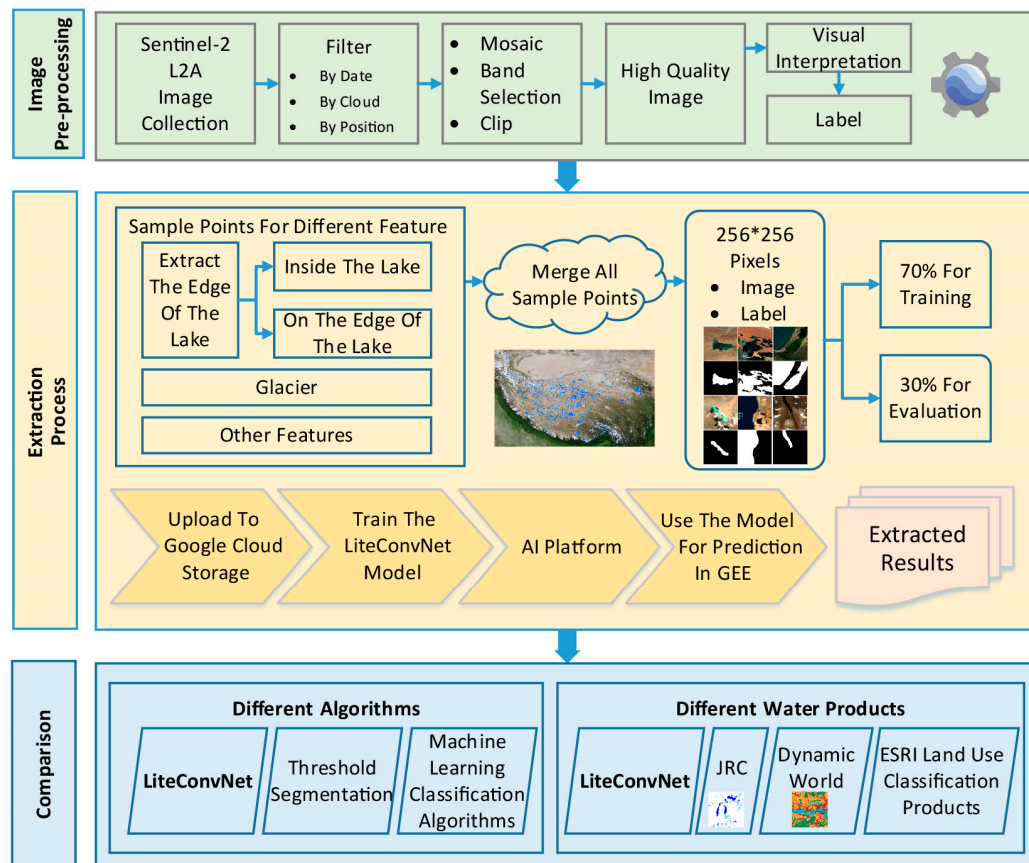


Figure 3. Overall workflow diagram.

2.3.1. Preparation of Sample Data

The representativeness of the samples used for deep learning significantly affects the results of lake identification. From one perspective, in the process of creating the dataset, we used only lakes as positive samples and other water bodies, such as river areas, as negative samples. We aimed to make the model concentrate on learning the morphological, textural, and spectral features of lakes by it training on these selected samples. This strategy was designed to enhance the model's accuracy in extracting lakes while effectively distinguishing them from other categories like rivers and glaciers with the help of the CNN's powerful learning capability. On the other side, if the sample points are randomly chosen within the region of interest, it tends to result in an imbalance between positive and negative samples. Some hard samples that could impact the classification of lakes are easily overlooked. Our suggested solution to this issue was a segmented method of sampling. Firstly, we used the existing water products to obtain the initial lake boundary. Secondly, samples were taken from both sides of the lake's edge. Thirdly, sample labels of 256×256 pixels were created centered on the sampling points. A schematic of using the edge of the lake to take sample points is shown in Figure 4.

This approach offers the following benefits. First of all, it enhances the assurance of maintaining an equilibrium between positive and negative examples. Secondly, there is an increased likelihood that the examples contain both water and non-water, rendering the examples more informative than single-water or -land examples. Thirdly, the inclusion of partially mixed target examples enhances the model's capacity to accurately detect

and classify targets, such as ice lakes. Subsequently, we amalgamated all the examples, allocating 70% for model training and 30% for validation. Training data samples are shown in Figure 5. We used the Google Colab platform to push examples in TFRecord format to Google Cloud Storage for subsequent investigation and analysis.

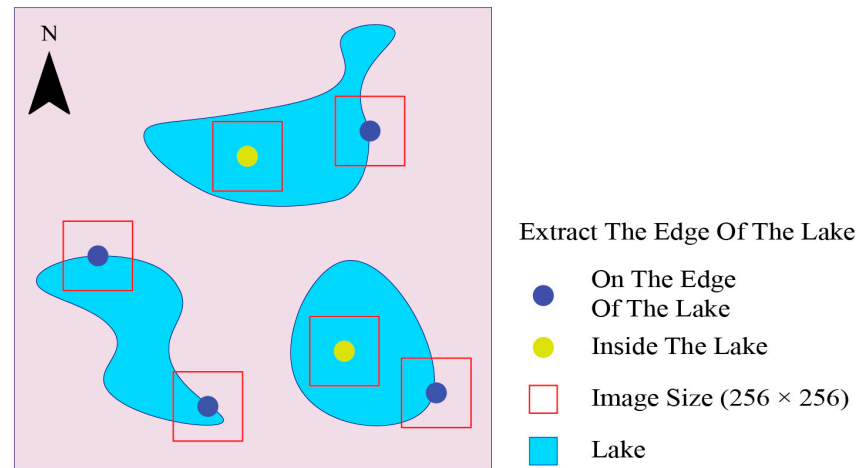


Figure 4. Schematic of using the edge of the lake to take sample points.

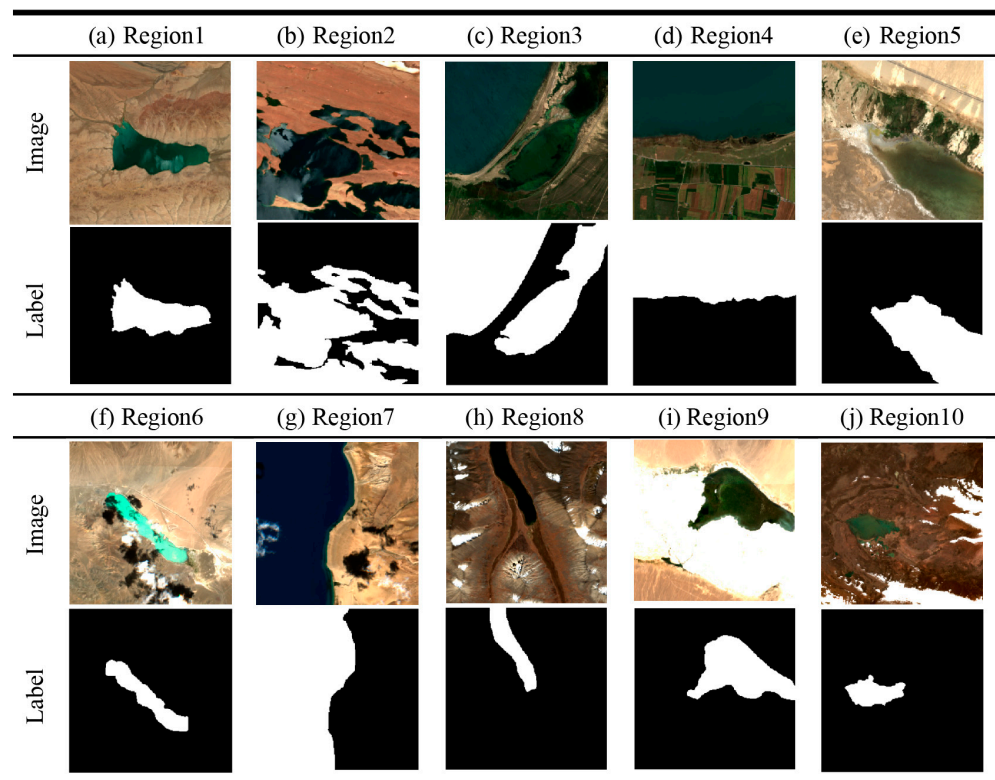


Figure 5. Training data samples.

2.3.2. Deep Learning Model and Training Model Architecture

Deep learning plays a crucial role in the field of computer vision and is extensively used in the analysis of remote sensing images [39,40]. The CNN is a powerful network architecture that demonstrates excellent performances in image recognition tasks [41].

To achieve real-time computation on the GEE platform, we propose a lightweight CNN named LiteConvNet to minimize model parameters. The LiteConvNet consists of

multiple convolution, batch normalization, dense, and activation layers. The architecture of the model is shown in Figure 6. The sizes of each convolutional kernel and feature map in the model are shown in Table 1. In addition, a 7×7 patch was used as input to obtain more spatial information and reduce the salt and pepper noise. Each 256×256 image was segmented into 7×7 patches before being fed into the model, and the category of the central pixel of each patch was considered the ground truth. The complete calculation process of LiteConvNet is described as follows.

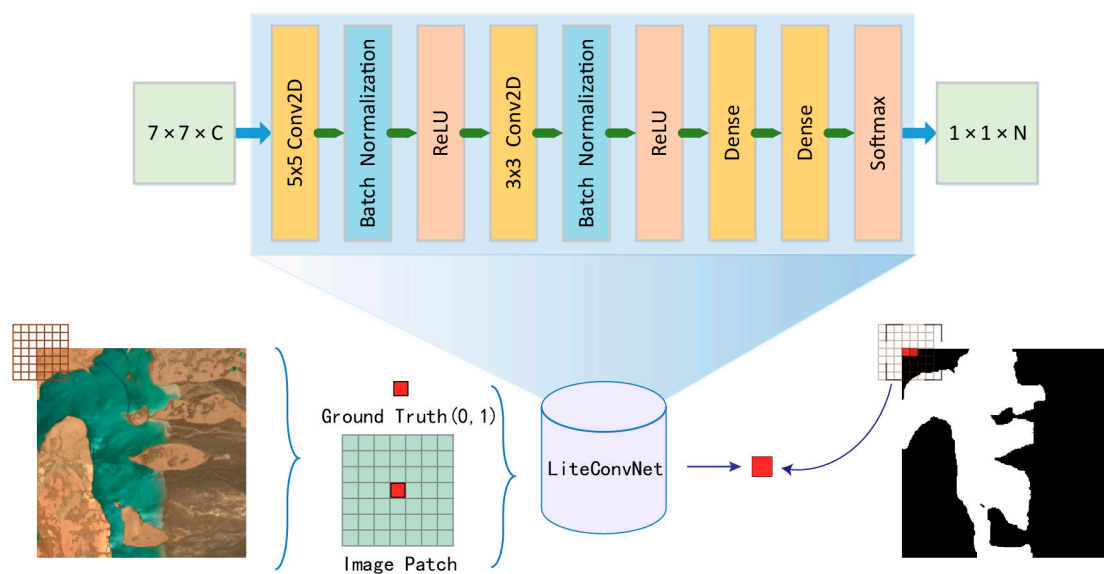


Figure 6. The architecture of the lightweight convolutional neural network (LiteConvNet).

Table 1. LiteConvNet model parameters.

Layer	Kernel Size	Output Shape	Param
Input Layer		(7, 7, 8)	0
Conv2D	5×5	(3, 3, 16)	3216
Batch Normalization		(3, 3, 16)	64
ReLU		(3, 3, 16)	0
Conv2D	3×3	(1, 1, 32)	4640
Batch Normalization		(1, 1, 32)	128
ReLU		(1, 1, 32)	0
Dense		(1, 1, 16)	528
Dense		(1, 1, 2)	34
Softmax		(1, 1, 2)	0

Firstly, the $7 \times 7 \times 8$ input data were processed into a $3 \times 3 \times 16$ feature map by a 5×5 convolutional layer with 16 filters, and then a batch normalization layer and a ReLU activation layer were employed to increase the nonlinear fitting ability of the model. Secondly, a 3×3 convolutional layer with 32 filters was used to repeat the first step's operation on the result, resulting in a $1 \times 1 \times 32$ feature map. Finally, two fully connected layers followed, generating new feature representations through linear combinations, and the output was transformed into a probability distribution using a Softmax activation layer.

This CNN model effectively captures the intricate details and structural characteristics of the image. To enhance feature extraction and realize real-time prediction, the approach involved dividing the input data into 7×7 patches. Compared to methods based on individual pixels, LiteConvNet uses 7×7 inputs, which results in a larger receptive field. This allows for a more comprehensive consideration of information from surrounding pixels, effectively capturing the pixel-level differences between lakes and other categories like rivers. The input data size and number of channels were also reduced, which effectively

reduced the number of parameters in the model, avoided overfitting problems, and reduced the computational complexity. In addition, the batch normalization layer enhances the stability and convergence speed of the model by normalizing the output of the convolutional layer. The activation function layer incorporates a non-linear modification, hence enhancing the network's expressiveness. The developed LiteConvNet model offers notable benefits in feature extraction, parameter optimization, stability, and expressiveness for image processing tasks. The model possesses the ability to autonomously acquire abstract concepts from unprocessed input and generate precise classification predictions based on these abstract notions.

Model Training and Deployment

Based on the TensorFlow framework, the LiteConvNet model was trained on Google Colab's Tesla P100 GPU. The experiment used the Adam optimizer and the categorical_crossentropy loss function. Training was performed for 30 epochs. In the process of building the model, we took full advantage of the Google Cloud Platform. Not only did we efficiently use the data stored in Cloud Storage to provide reliable data support for the model training, but also by leveraging the excellent environment provided by the Google Cloud Platform, we achieved the online training, deployment, and management of the models. Once the models were trained, we pushed them to the AI Platform to further improve the availability and deployment efficiency of the models. In the next step, we were able to launch the trained model directly on the GEE platform, which provided us with the conditions for lake extraction on the Tibetan Plateau.

2.3.3. Evaluation Metrics

The primary model employed in the ALEW process of the study's experimental setup was the LiteConvNet model, which was used to accurately extract lakes across the Tibetan Plateau. To assess the reliability of the LiteConvNet model in identifying lakes on the Tibetan Plateau, we employed precision assessment measures to analyze the outcomes. The measures encompass the Precision, Recall, F1-score, Intersection over Union (IoU), Overall Accuracy (OA), and mean Intersection over Union (MIoU). The formulas for these metrics are as follows:

$$\text{Precision} = \frac{TP}{TP + FP} \quad (1)$$

$$\text{Recall} = \frac{TP}{TP + FN} \quad (2)$$

$$\text{F1 - score} = \frac{2 \times \text{Precision} \times \text{Recall}}{\text{Precision} + \text{Recall}} \quad (3)$$

$$\text{IoU} = \frac{TP}{TP + FN + FP} \quad (4)$$

$$\text{OA} = \frac{TP + TN}{TP + TN + FN + FP} \quad (5)$$

$$\text{MIoU} = \frac{\frac{TP}{TP+FN+FP} + \frac{TN}{TN+FN+FP}}{2} \quad (6)$$

These metrics provide a comprehensive assessment of model performance, measuring the accuracy and error of classification results from different perspectives. Among them, TP represents true positive, FP represents false positive, FN represents false negative, and TN represents true negative. These metrics offer a thorough evaluation of model performance and quantify the precision of categorization outcomes from several viewpoints. We also conducted a full evaluation of the LiteConvNet model's performance by comparing it with other common threshold segmentation methods, traditional machine learning, and a number of open-source classification products. This was accomplished through both visual

and quantitative evaluation methods. Additionally, we analyzed the efficacy of several approaches on the task of identifying lakes.

3. Results

3.1. Lake Extraction Results

ALEW demonstrates notable benefits in the task of identifying lakes on the Tibetan Plateau by integrating cloud computing, deep learning, and remote sensing big data. The model can effectively handle extensive remote sensing data by invoking the previously trained CNN model on the AI platform within the GEE platform. It is worth mentioning that it only takes less than 5 min to obtain the lake extraction results for the entire Tibetan Plateau using the ALEW process. The model was applied to predict on Sentinel-2 images and generate the probability value of a lake. By establishing an appropriate threshold, we converted the probability values into binary results, where a value of one signifies extraction as a lake. The map of lake extraction results on the Tibetan Plateau is shown in Figure 7. Using the LiteConvNet model, we could see that by accurately extracting the shapes of various lakes, the model learns complex features from the images, enhancing its ability to generalize between different lakes throughout the Tibetan Plateau.

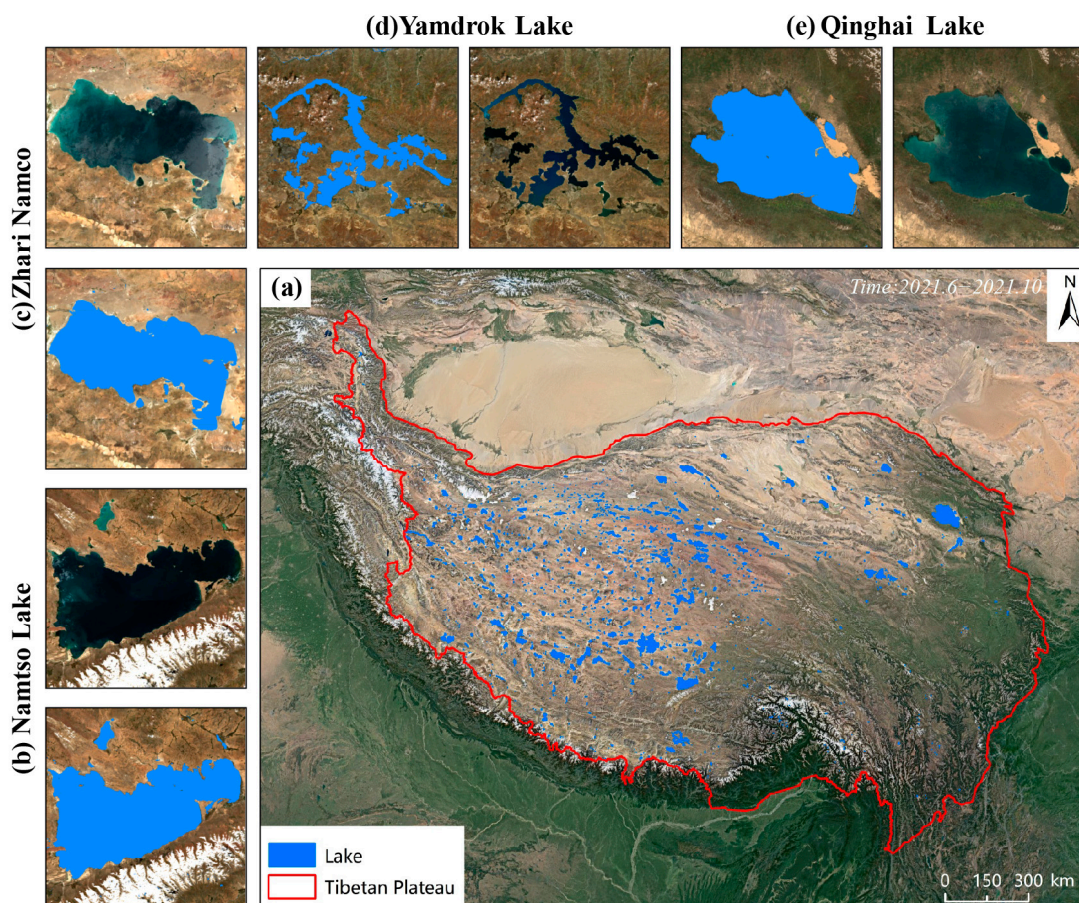


Figure 7. Maps of lake extraction results on the Tibetan Plateau.

The diversity and complexity of lakes on the Tibetan Plateau can be seen through the results. The large number of lakes and their wide distribution create conditions for the formation of rich lake ecosystems. The percentage of lake areas on the Tibetan Plateau in different ranges is shown in Figure 8. The results show that there are a large number of small lakes on the Tibetan Plateau, especially lakes smaller than 5 square kilometers, which occupy more than half of the total number of lakes. However, the major proportion of lake area is occupied by lakes with an area range of $(100.0 \leq \text{Area} < 250.0, 250.0 \leq \text{Area} < 1000.0,$

Area ≥ 1000.0), which accounted for about 70% of the average total area of the lakes. It shows the unevenness of the distribution of lake area. Small lakes form the basis of the number of lakes, while large lakes dominate the total area. In addition, using the data on the same region published by the National Tibetan Plateau Data Center [42] for comparison, there is a high degree of consistency in the range of area distribution. The statistical difference in the area of lakes over 1 square kilometer between the two is about 2%. In terms of details, we chose to investigate four lakes, which are as follows: Namtso Lake, Qinghai Lake, Yamdrok Lake, and Zhari Namco. The lakes' extraction outcomes show off the LiteConvNet model's robustness in the lake extraction task as well as its precision in capturing the lakes' contours and intricate details. It shows off the model's superb detail-capturing capabilities. The convolutional layer automatically captures the abstract features of the lake by learning the spatial hierarchy in the image, while the pooling layer helps to reduce the dimensionality of the feature map, improving computational efficiency while retaining key information. The hierarchical feature learning process helps to better understand the morphology and distribution of lakes. The LiteConvNet model exhibits strong learning and generalization capabilities through distributed computing on the GEE platform, allowing it to adapt to lake extraction tasks under varying geographical environments and data characteristics. Simultaneously, the model effectively employs high-performance computing resources to automate the extraction process of lakes, thereby offering dependable support for lake surveillance and ecological environment studies.

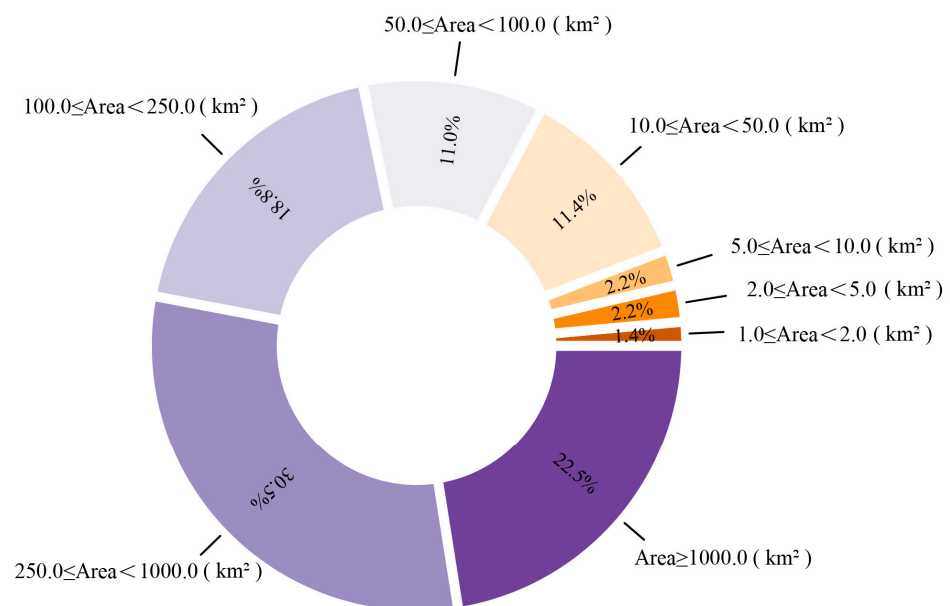


Figure 8. Percentages of lake areas on the Tibetan Plateau in different ranges.

3.2. Results of Ablation Experiments

In convolutional neural networks, the size of the convolutional kernel determines the receptive field of the neuron on the input image, which affects the ability of the model to capture spatial information. This work set up two sets of ablation experiments with input 3×3 and 1×1 image sizes for comparison in order to demonstrate the impact of different input sizes on the model results.

LiteConvNet (3×3) contains only one 1×1 convolutional layer. While this setup reduces the amount of computation and number of parameters, it also reduces the expressive power and overall performance of the network, with an accuracy of 0.9688 and a mIoU of 0.9377. On the other hand, LiteConvNet (1×1) uses the 1×1 size directly, with an accuracy of 0.9619 and an IOU of 0.9288. A comparison of accuracy for different extraction methods in LiteConvNet is shown in Table 2. In contrast, LiteConvNet (7×7) captures more spatial information, and the model determines the class of the central pixel from

the 7×7 surrounding pixels. This reduces the false positive rate by determining more accurately whether the target is a body of water than the pixel calculation. This means that LiteConvNet (7×7) can improve on the pretzel effect of traditional machine learning methods based on pixel classification. By using a 3×3 convolutional kernel, it can further extract features, which improves the accuracy of feature classification and contributes to the better recognition of fine-grained features. The 5×5 and 3×3 convolutional kernels used in LiteConvNet (7×7) enable more efficient image processing compared to relatively large convolutional kernels, especially when resources are limited. The size of the convolutional kernel affects the feature extraction and model representation of the network. Larger convolutional kernels can capture more complex image patterns and abstract feature representations, but too large a convolutional kernel may also lead to model overfitting or over-reliance on global data. In contrast, smaller convolutional kernels can be stacked multiple times to extract the same range of features, which allows the model to better perceive local features. In addition, larger convolutional kernels have better nonlinear expressiveness due to having more free parameters, whereas smaller convolutional kernels may limit the expressiveness of the model due to the smaller number of parameters. Therefore, in order to ensure that the convolutional neural network can adequately fit the training data and, at the same time, have a better generalization performance, the relationship between the number of parameters and the expressive ability needs to be balanced.

Table 2. Comparison of accuracy for different extraction methods in LiteConvNet.

	Precision	Recall	F1-Score	IoU	OA	MIoU
LiteConvNet (7×7)	0.9730	0.9739	0.9735	0.9483	0.9744	0.9483
LiteConvNet (3×3)	0.9688	0.9669	0.9678	0.9377	0.9688	0.9377
LiteConvNet (1×1)	0.9619	0.9642	0.9630	0.9288	0.9643	0.9288

The results of the experiments show that the LiteConvNet (7×7) model works well for finding lakes, which also shows that the right choice of convolutional kernel sizes is important. The 5×5 and 3×3 convolutional kernels used in LiteConvNet (7×7) help to improve the performance of remote sensing image processing tasks. LiteConvNet (7×7) works better at remote sensing image processing tasks. It can improve the accuracies in remote sensing image classification and segmentation tasks by improving the sensing field, feature extraction, and model representation. This is accomplished using settings and different convolutional kernel sizes and dimensions that fit the needs of the task. At the same time, it can be adapted to various computational and storage requirements. As a result, the LiteConvNet (7×7) model performs better at identifying lakes.

4. Discussion

4.1. Comparison of Different Extraction Methods

To assess the efficacy of the GEE platform and the ALEW method in this domain and enhance the precision and efficiency of lake extraction, we employed the LiteConvNet model in a comparative analysis against the conventional approach. Utilizing the GEE platform, we employed the LiteConvNet model's remote sensing images as input. By applying the NDWI index and conducting a visual observation, we performed lake extraction through the selection of an appropriate threshold. Machine learning techniques have become extensively employed for the purpose of water body extraction in recent times. Random forest (RF) is a common remote sensing image classification method that has a higher accuracy and stability than the traditional threshold segmentation method. By constructing multiple decision trees, RF can automatically learn the features and thresholds to reduce the interference of human factors [43].

Following extensive testing, the LiteConvNet model successfully produced favorable outcomes in the extraction of lakes in the Tibetan Plateau region. Figure 9 illustrates that the LiteConvNet model achieves an OA of 0.9744 and an F1-score of 0.9730. This

is a significant increase when compared to the RF and NDWI methods. In this region characterized by intricate topography and diverse weather patterns, the conventional threshold segmentation method employing the NDWI index, as well as traditional machine learning techniques such as RF, encounter specific challenges in accurately extracting lakes and distinguishing them from their surrounding areas. Compared to the traditional threshold segmentation method, the deep learning algorithm is able to analyze the image based on its information and no longer relies on a fixed threshold. Thus, LiteConvNet is more effective in handling areas with significant variations in spectral characteristics and prevents the inadequate capture of lake shapes in the threshold segmentation approach. LiteConvNet possesses the ability to adjust to the complex terrain and changes in the features of remote sensing images. It can efficiently make use of the informational attributes of remote sensing images to uncover underlying patterns within the image and identify distinguishing features that separate lakes from other elements.

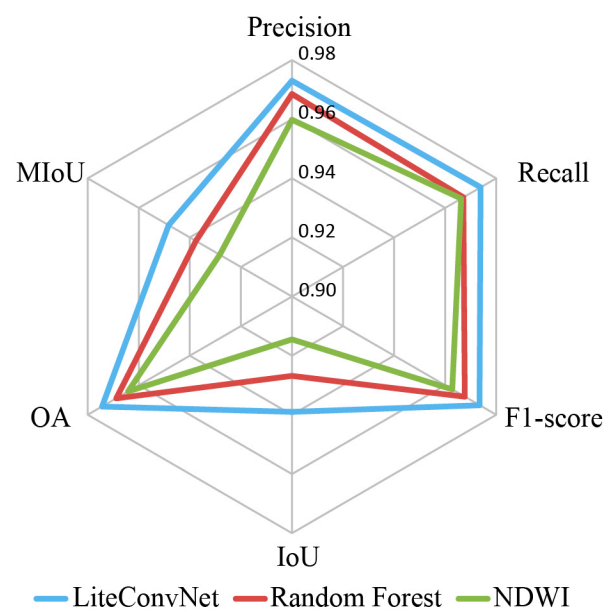


Figure 9. Comparison of the accuracies for extraction methods LiteConvNet, Random Forest, and normalized difference water index (NDWI).

While RF can effectively identify lakes, it may mistakenly identify shadows as water bodies in challenging terrain. Additionally, it is also unable to distinguish lakes and rivers, and there is a certain amount of noise interference in the classification results. Compared to the RF model, LiteConvNet performs better in separating lake and river boundaries and is able to more accurately delineate the boundaries of lakes and rivers by effectively integrating multiple layers of information, including features in multiple dimensions such as spectra, texture, and shape. Compared to the traditional threshold segmentation method, the deep learning algorithm is able to analyze the image based on its information and no longer relies on a fixed threshold. Therefore, LiteConvNet can better deal with regions with large spectral differences and avoid the incomplete extraction of lake morphology in the threshold segmentation method. A comparison of LiteConvNet, RF, and NDWI extraction methods is shown in Figure 10. LiteConvNet has the ability to adapt to the complex terrain and changes in the features of remote sensing images, and it can effectively use the information features of remote sensing images to dig into the deeper laws of the image and find effective features to distinguish water bodies from other features.

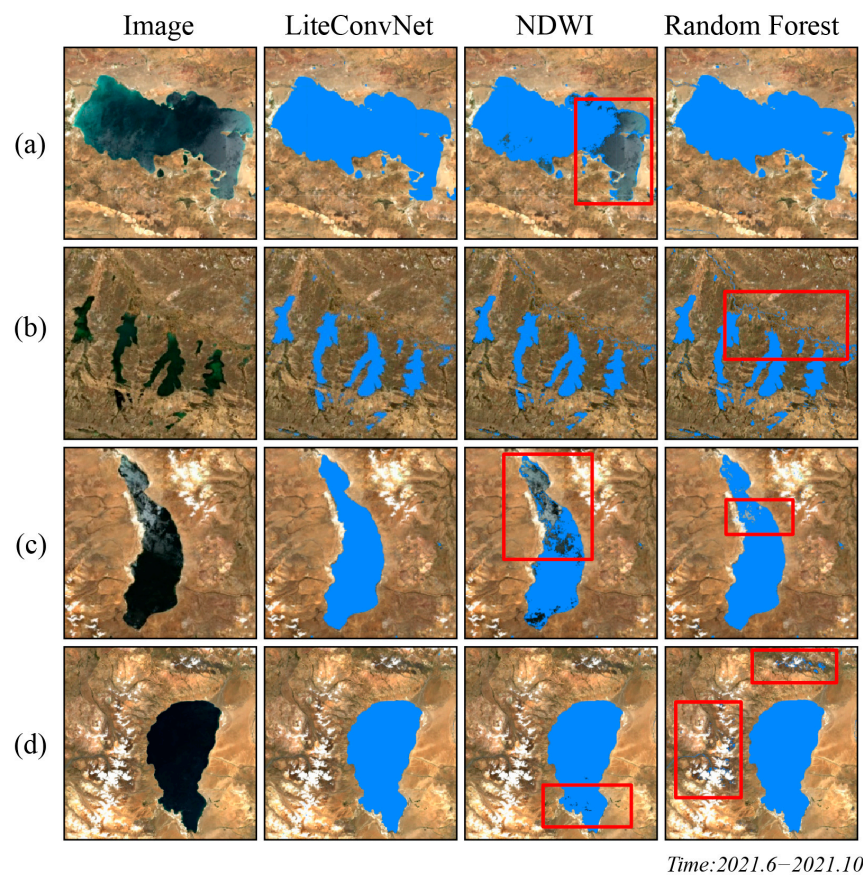


Figure 10. Comparison of the LiteConvNet, Random Forest, and NDWI extraction methods. Subfigures (a–d) are detailed representations of the different lakes on the Tibetan Plateau. The red circles stand for regions where the extraction performance is not optimal.

4.2. Comparison of Different Water Products

In this study, considering the inadequacy of existing lake extraction products on the Tibetan Plateau, we selected the JRC Monthly Water History dataset (JRC) as well as water products from Dynamic World and ESRI 10 m Annual Land Use Land Cover (ESRI) for comparison [44–46]. It is of great significance for evaluating the LiteConvNet model in the ALEW process for lake identification. The introduction of different water products is shown in Table 3.

Table 3. The introduction of different water products.

Dataset	Abbreviation	Dataset ID in GEE	Images	Time Range	Spatial Resolution
JRC Monthly Water History dataset	JRC	JRC/GSW1_4/MonthlyHistory	Landsat5.7.8	June–October 2021	30 m
Dynamic World	Dynamic World	GOOGLE/DYNAMICWORLD/V1	Sentinel-2	June–October 2021	10 m
ESRI 10 m Annual Land Use Land Cover	ESRI	projects/sat-io/open-datasets/landcover/ESRI_Global-LULC_10 m	Sentinel-2	2021	10 m

We choose four regions on the Tibetan Plateau. Figure 11 illustrates LiteConvNet’s extraction results and water products in comparison with the label. Blue represents the same regions, red represents deficient regions, and green represents excessive regions. The experimental results demonstrate the excellent performance of the LiteConvNet model when dealing with the task of lake extraction in complex situations. The results of LiteConvNet

are in good agreement with the existing three types of water products, but the LiteConvNet model has a more obvious advantage in the accurate extraction of lakes. As the complete dataset covers a variety of lake scenarios, it allows the model to comprehensively learn and extract key features of lakes. At the same time, the model was specifically optimized to discriminate between lakes and rivers. This enables it to exhibit better adaptability and accuracy in large-scale lake monitoring, providing a new perspective on lake monitoring research. The model is significantly enhanced in its ability to analyze and process multi-band image data through its lightweight convolutional network architecture, making it possible to identify the spectral information of lakes and accurately define the extent of lakes. Although the results on the Dynamic World data are acceptable on a large scale, the accuracy of the extraction at the edges of the lake is relatively low, and in some areas there may be missed identifications. We observed that the ESRI classification results expand the lake's extent in a circular manner. LiteConvNet demonstrates an extremely high level of detail in the handling of lake edge features, as can be seen in its performance in accurately capturing lake shorelines and subtle changes. By effectively using high-resolution data, LiteConvNet shows significant superiority in spatial resolution, which captures the fine features of lakes in greater detail.

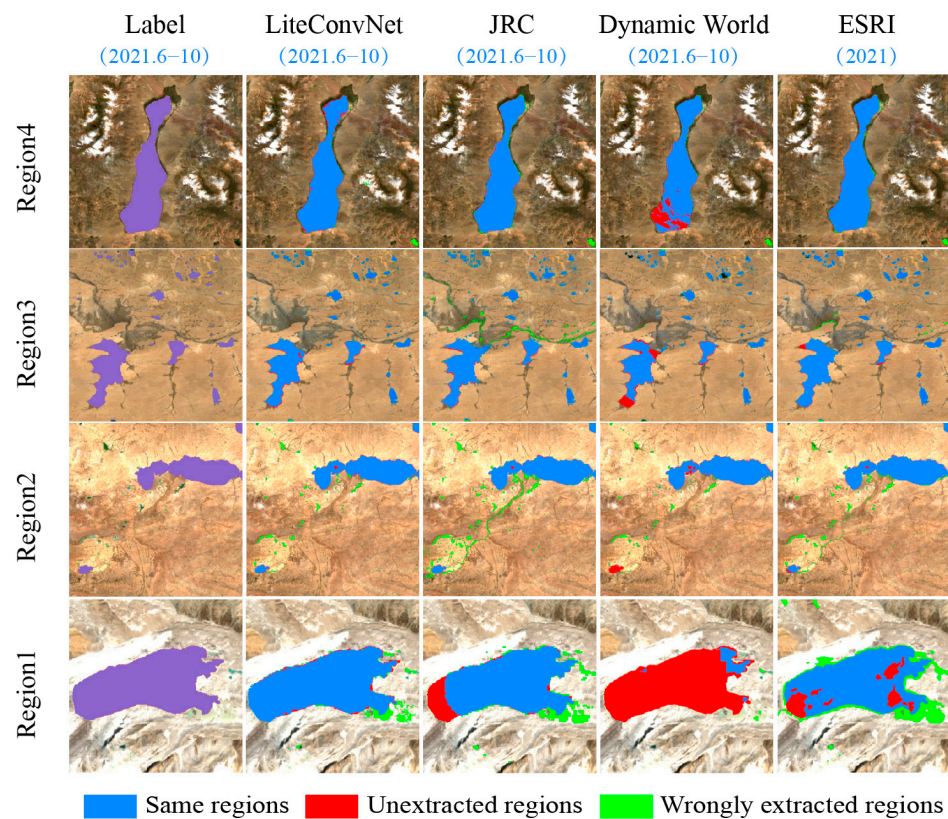


Figure 11. LiteConvNet extraction results and water products in comparison with the label.

We assessed the accuracy of the extraction results obtained by the LiteConvNet model compared with different water products in terms of visual interpretation and quantitative analysis. The results indicate that the LiteConvNet model demonstrates a higher accuracy in extracting data from a lake's border. It efficiently captures water bodies across various time intervals, thereby avoiding any erroneous extraction of a river. The ALEW approach is an ideal solution for accurately extracting lakes in difficult terrain. This is of crucial practical value for investigating, monitoring, and conserving water resources in the Tibetan Plateau.

4.3. Limitation

In order to achieve the accurate extraction of lakes on a wide range of scales, this paper took the Tibetan Plateau as the study area and proposed the Automated Lake Extraction Workflow by combining deep learning, and the LiteConvNet model in ALEW has a strong recognition ability in lakes. The method can effectively extract lakes on a wide-area scale, but there are still some aspects that need further research and improvement in this study. (1) Efforts to mitigate the exorbitant expenditure. Given the constraints of the Google Cloud Platform, utilizing it for an extended period of time incurs significant costs. One way to further investigate this issue is by attempting to modify the network architecture of deep learning in order to minimize the reliance on computational resources, thereby decreasing the overall expenses. (2) Further optimization of the deep learning model to improve its capacity for distinguishing lakes from other aquatic formations. Although the LiteConvNet model can effectively partition water bodies from lakes, it now does not possess the capacity to fully distinguish between them. Subsequent investigations could explore the integration of the semantic segmentation model with the GEE platform to enhance the model's ability to acquire novel characteristics and generate precise images that capture intricate contextual details. This integration has the potential to enhance precision in differentiating aquatic bodies from lakes. (3) Study of changes in lakes on the Tibetan Plateau over a long time series. Recently, due to climate warming and increased humidity, there have been incidents such as the sudden eruption of Zhuonai Lake and the overflowing of the Salt Lake on the Tibetan Plateau. These events have had a significant impact on human life and ecological balance. Therefore, it is crucial to maintain a continuous monitoring of the lakes. It is necessary to expand the entire procedure to a lengthy time series in order to monitor the lakes on the Tibetan Plateau. This will offer technical support in advancing the conservation, management, and disaster prevention of these lakes.

5. Conclusions

The innovation of this article is that we propose the ALEW process based on the GEE cloud platform and deep learning, which aims to extract lake information from images over a wide area. The ALEW process utilizes the GEE platform, eliminating the need for the extensive pre-processing and downloading of images. By just writing appropriate code, the image data may be swiftly processed and analyzed. With the powerful computing power and rich data collection of the GEE platform, the remote sensing inversion work becomes more efficient and accurate. It took less than 5 min to obtain the lake extraction results for the entire Tibetan Plateau using the ALEW process. Furthermore, by leveraging the formidable capabilities of the Google Cloud Platform in conjunction with deep learning, the proposed workflow can rapidly identify targets across a vast expanse and provide strong support for research work.

In this study, we constructed the LiteConvNet model to ensure inference efficiency under the premise of obtaining better lake extraction results, and we innovated the segmented sampling method, which provides a new solution for setting sampling points for lakes on a large scale. A lake extraction dataset was created on the Tibetan Plateau to train the LiteConvNet model using the GEE platform. The results demonstrate that the LiteConvNet model may greatly enhance the precision of lake extraction in complex situations, achieving an overall accuracy of 97.44%. The LiteConvNet model demonstrates a superior accuracy in identifying lake information from images when compared to the threshold segmentation method and RF results. This demonstrates the effectiveness of the method in extracting precise and reliable information about lakes across a wide geographical region. In order to ascertain the superiority of the recognition findings, we conducted a comparison using the JRC dataset, Dynamic World, and ESRI's categorization products. The method clearly demonstrates superior accuracy in extracting lake boundaries, as well as possessing a greater spatial resolution. Additionally, it is capable of precisely identifying water bodies across various time scales while effectively avoiding any misidentification of rivers.

The ALEW method, proposed in this paper, offers a means to dynamically monitor lakes in a wide range of areas. This method aids in analyzing the patterns and causes of spatial and temporal changes in lake areas. It also facilitates the automation and intelligence of monitoring plateau lakes over extended time periods. Moreover, it provides technical and data support for studying the ecological environment of plateau lakes. It also holds significant theoretical and practical importance in developing the response model for lake changes in relation to climate change, the regional water balance model, and the forecast of climate change. In addition, it can elucidate the influence of worldwide alterations on local ecological transformations and provide a scientific foundation for ensuring ecological and environmental security, socio-economic progress, administration, and strategic decision making.

Author Contributions: Conceptualization, J.Y. and Y.P.; methodology, J.Y.; software, P.Z.; validation, Y.P. and L.X.; formal analysis, P.H.; investigation, L.X.; resources, P.H.; data curation, L.Z.; writing—original draft preparation, Y.P.; writing—review and editing, J.Y.; visualization, L.X.; supervision, C.H.; project administration, D.G.; funding acquisition, D.G. All authors have read and agreed to the published version of the manuscript.

Funding: This research was funded by the National Key Research and Development Program of China (2021YFC3000400).

Data Availability Statement: The data presented in this study are available on request from the corresponding author.

Conflicts of Interest: The authors declare no conflicts of interests.

References

1. Woolway, R.I.; Kraemer, B.M.; Leters, J.D.; Merchant, C.J.; O'Reilly, C.M.; Sharma, S. Global lake responses to climate change. *Nat. Rev. Earth Environ.* **2020**, *1*, 388–403. [\[CrossRef\]](#)
2. Liu, E.; Yang, X.; Shen, J.; Dong, X.; Zhang, E.; Wang, S. Environmental response to climate and human impact during the last 400 years in Taibai Lake catchment, middle reach of Yangtze River, China. *Sci. Total Environ.* **2007**, *385*, 196–207. [\[CrossRef\]](#) [\[PubMed\]](#)
3. Xiong, F.; Chen, Y.; Zhang, S.; Xu, Y.; Lu, Y.; Qu, X.; Gao, W.; Wu, X.; Xin, W.; Gang, D.D.; et al. Land use, hydrology, and climate influence water quality of China's largest river. *J. Environ. Manag.* **2022**, *318*, 115581. [\[CrossRef\]](#) [\[PubMed\]](#)
4. Beeton, A.M. Large freshwater lakes: Present state, trends, and future. *Environ. Conserv.* **2002**, *29*, 21–38. [\[CrossRef\]](#)
5. Wrigley, R.C.; Horne, A.J. Remote sensing and lake eutrophication. *Nature* **1974**, *250*, 213–214. [\[CrossRef\]](#)
6. Roy, P.S.; Behera, M.D.; Srivastav, S.K. Satellite remote sensing: Sensors, applications and techniques. *Proc. Natl. Acad. Sci. India Sect. A Phys. Sci.* **2017**, *87*, 465–472. [\[CrossRef\]](#)
7. McFeeters, S.K. The use of the Normalized Difference Water Index (NDWI) in the delineation of open water features. *Int. J. Remote Sens.* **1996**, *17*, 1425–1432. [\[CrossRef\]](#)
8. Xu, H. A study on information extraction of water body with the modified normalized difference water index (MNDWI). *J. Remote Sens.* **2005**, *9*, 595.
9. Wang, Q.; Liu, D.; Yang, H.; Yin, J.; Bin, Z.; Zhu, S.; Zhang, Y. Comparative study on the water index of MNDWI and NDWI for water boundary extraction in eutrophic lakes. *Adv. Geosci.* **2017**, *7*, 732–738. [\[CrossRef\]](#)
10. Deoli, V.; Kumar, D.; Kuriqi, A. Detection of water spread area changes in eutrophic lake using landsat data. *Sensors* **2022**, *22*, 6827. [\[CrossRef\]](#)
11. Tran, K.H.; Menenti, M.; Jia, L. Surface Water Mapping and Flood Monitoring in the Mekong Delta Using Sentinel-1 SAR Time Series and Otsu Threshold. *Remote Sens.* **2022**, *14*, 5721. [\[CrossRef\]](#)
12. Sarp, G.; Ozcelik, M. Water body extraction and change detection using time series: A case study of Lake Burdur, Turkey. *J. Taibah Univ. Sci.* **2017**, *11*, 381–391. [\[CrossRef\]](#)
13. Nhu, V.H.; Shahabi, H.; Nohani, E.; Shirzadi, A.; Al-Ansari, N.; Bahrami, S.; Miraki, S.; Geertsema, M.; Nguyen, H. Daily water level prediction of Zrebar Lake (Iran): A comparison between M5P, random forest, random tree and reduced error pruning trees algorithms. *ISPRS Int. J. Geo-Inf.* **2020**, *9*, 479. [\[CrossRef\]](#)
14. Yu, L.; Wang, Z.; Tian, S.; Ye, F.; Ding, J.; Kong, J. Convolutional neural networks for water body extraction from Landsat imagery. *Int. J. Comput. Intell.* **2017**, *16*, 1750001. [\[CrossRef\]](#)
15. Wang, Z.; Gao, X.; Zhang, Y.; Zhao, G. MSLWENet: A novel deep learning network for lake water body extraction of Google remote sensing images. *Remote Sens.* **2020**, *12*, 4140. [\[CrossRef\]](#)
16. Gorelick, N.; Hancher, M.; Dixon, M.; Ilyushchenko, S.; Thau, D.; Moore, R. Google Earth Engine: Planetary-scale geospatial analysis for everyone. *Remote Sens. Environ.* **2017**, *202*, 18–27. [\[CrossRef\]](#)

17. Tamiminia, H.; Salehi, B.; Mahdianpari, M.; Quackenbush, L.; Adeli, S.; Brisco, B. Google Earth Engine for geo-big data applications: A meta-analysis and systematic review. *ISPRS J. Photogramm. Remote Sens.* **2020**, *164*, 152–170. [[CrossRef](#)]
18. Amani, M.; Ghorbanian, A.; Ahmadi, S.A.; Kakooei, M.; Moghimi, A.; Mirmazloumi, S.M.; Moghaddam, S.H.A.; Mahdavi, S.; Ghahremanloo, M.; Parsian, S.; et al. Google earth engine cloud computing platform for remote sensing big data applications: A comprehensive review. *IEEE J. Sel. Top. Appl. Earth Obs. Remote Sens.* **2020**, *13*, 5326–5350. [[CrossRef](#)]
19. Hansen, M.C.; Potapov, P.V.; Moore, R.; Hancher, M.; Turubanova, S.A.; Tyukavina, A.; Thau, D.; Stehman, S.V.; Goetz, S.J.; Loveland, T.R.; et al. High-resolution global maps of 21st-century forest cover change. *Science* **2013**, *342*, 850–853. [[CrossRef](#)]
20. Yan, Y.; Zhuang, Q.; Zan, C.; Ren, J.; Yang, L.; Wen, Y.; Zeng, S.; Zhang, Q.; Kong, L. Using the Google Earth Engine to rapidly monitor impacts of geohazards on ecological quality in highly susceptible areas. *Ecol Indic.* **2021**, *132*, 108258. [[CrossRef](#)]
21. Zhao, Z.; Islam, F.; Waseem, L.A.; Tariq, A.; Nawaz, M.; Islam, I.U.; Bibi, T.; Rehman, N.U.; Ahmad, W.; Aslam, R.W.; et al. Comparison of Three Machine Learning Algorithms Using Google Earth Engine for Land Use Land Cover Classification. *Rangeland Ecol. Manag.* **2024**, *92*, 129–137. [[CrossRef](#)]
22. Liu, X.; Hu, G.; Chen, Y.; Li, X.; Xu, X.; Li, S.; Pei, F.; Wang, S. High-resolution multi-temporal mapping of global urban land using Landsat images based on the Google Earth Engine Platform. *Remote Sens. Environ.* **2018**, *209*, 227–239. [[CrossRef](#)]
23. Sturrock, H.J.; Cohen, J.M.; Keil, P.; Tatem, A.J.; Le Menach, A.; Ntshalintshali, N.E.; Hsiang, M.S.; Gosling, R.D. Fine-scale malaria risk mapping from routine aggregated case data. *Malar. J.* **2014**, *13*, 421. [[CrossRef](#)] [[PubMed](#)]
24. Cai, Y.; Guan, K.; Peng, J.; Wang, S.; Seifert, C.; Wardlow, B.; Li, Z. A high-performance and in-season classification system of field-level crop types using time-series Landsat data and a machine learning approach. *Remote Sens. Environ.* **2018**, *210*, 35–47. [[CrossRef](#)]
25. Wang, Y.; Ma, J.; Xiao, X.; Wang, X.; Dai, S.; Zhao, B. Long-term dynamic of Poyang Lake surface water: A mapping work based on the Google Earth Engine cloud platform. *Remote Sens.* **2019**, *11*, 313. [[CrossRef](#)]
26. Sha, T.; Yao, X.; Wang, Y.; Tian, Z. A Quick Detection of Lake Area Changes and Hazard Assessment in the Qinghai–Tibet Plateau Based on GEE: A Case Study of Tuosu Lake. *Front. Earth Sci.* **2022**, *10*, 934033. [[CrossRef](#)]
27. Li, J.; Peng, B.; Wei, Y.; Ye, H. Accurate extraction of surface water in complex environment based on Google Earth Engine and Sentinel-2. *PLoS ONE* **2021**, *16*, e0253209. [[CrossRef](#)] [[PubMed](#)]
28. Chen, F.; Zhang, M.; Tian, B.; Li, Z. Extraction of glacial lake outlines in Tibet Plateau using Landsat 8 imagery and Google Earth Engine. *IEEE J. Sel. Top. Appl. Earth Obs. Remote Sens.* **2017**, *10*, 4002–4009. [[CrossRef](#)]
29. Zhang, M.; Chen, F.; Guo, H.; Yi, L.; Zeng, J.; Li, B. Glacial Lake area changes in high mountain asia during 1990–2020 using satellite remote sensing. *Research* **2022**, *2022*, 9821275. [[CrossRef](#)]
30. Wang, Y.; Li, Z.; Zeng, C.; Xia, G.S.; Shen, H. An urban water extraction method combining deep learning and Google Earth engine. *IEEE J. Sel. Top. Appl. Earth Obs. Remote Sens.* **2020**, *13*, 769–782. [[CrossRef](#)]
31. Mayer, T.; Poortinga, A.; Bhandari, B.; Nicolau, A.P.; Markert, K.; Thwal, N.S.; Markert, A.; Haag, A.; Kilbride, J.; Chishtie, F.; et al. Deep learning approach for Sentinel-1 surface water mapping leveraging Google Earth Engine. *ISPRS J. Photogramm. Remote Sens.* **2021**, *2*, 100005. [[CrossRef](#)]
32. Li, K.; Wang, J.; Cheng, W.; Wang, Y.; Zhou, Y.; Altansukh, O. Deep learning empowers the Google Earth Engine for automated water extraction in the Lake Baikal Basin. *Int. J. Appl. Earth Obs. Geoinf.* **2022**, *112*, 102928. [[CrossRef](#)]
33. Shen, M.; Wang, S.; Jiang, N.; Sun, J.; Cao, R.; Ling, X.; Fang, B.; Zhang, L.; Xu, X.; et al. Plant phenology changes and drivers on the Qinghai–Tibetan Plateau. *Nat. Rev. Earth Environ.* **2022**, *3*, 633–651. [[CrossRef](#)]
34. Zhang, G.; Yao, T.; Xie, H.; Yang, K.; Zhu, L.; Shum, C.K.; Bolch, T.; Yi, S.; Allen, S.; Jiang, L.; et al. Response of Tibetan Plateau lakes to climate change: Trends, patterns, and mechanisms. *Earth-Sci. Rev.* **2020**, *208*, 103269. [[CrossRef](#)]
35. Zhang, Y.; Ren, H.; Pan, X. *Integration Dataset of Tibet Plateau Boundary*; National Tibetan Plateau Data Center: Beijing, China, 2019.
36. Liu, L.; Xiao, X.; Qin, Y.; Wang, J.; Xu, X.; Hu, Y.; Qiao, Z. Mapping cropping intensity in China using time series Landsat and Sentinel-2 images and Google Earth Engine. *Remote Sens. Environ.* **2020**, *239*, 111624. [[CrossRef](#)]
37. Garajeh, M.K.; Malakyar, F.; Weng, Q.; Feizizadeh, B.; Blaschke, T.; Lakes, T. An automated deep learning convolutional neural network algorithm applied for soil salinity distribution mapping in Lake Urmia, Iran. *Sci. Total Environ.* **2021**, *778*, 146253. [[CrossRef](#)] [[PubMed](#)]
38. Li, Y.; Xie, W.; Li, H. Hyperspectral image reconstruction by deep convolutional neural network for classification. *Pattern Recogn.* **2017**, *63*, 371–383. [[CrossRef](#)]
39. Nogueira, K.; Penatti, O.A.; Dos Santos, J.A. Towards better exploiting convolutional neural networks for remote sensing scene classification. *Pattern Recogn.* **2017**, *61*, 539–556. [[CrossRef](#)]
40. Li, Z.; Liu, F.; Yang, W.; Peng, S.; Zhou, J. A survey of convolutional neural networks: Analysis, applications, and prospects. *IEEE Trans. Neural Netw. Learn. Syst.* **2021**, *33*, 6999–7019. [[CrossRef](#)]
41. Pan, X.; Zhao, J. A central-point-enhanced convolutional neural network for high-resolution remote-sensing image classification. *Int. J. Remote Sens.* **2017**, *38*, 6554–6581. [[CrossRef](#)]
42. Zhang, G. *The Lakes Larger than 1 km² in Tibetan Plateau (v3.1) (1970s–2022)*; Third Pole Environment Data Center (TPDC) : Beijing, China, 2019; Volume 10.
43. Phan, T.N.; Kuch, V.; Lehnert, L.W. Land cover classification using Google Earth Engine and random forest classifier—The role of image composition. *Remote Sens.* **2020**, *12*, 2411. [[CrossRef](#)]

44. Pekel, J.F.; Cottam, A.; Gorelick, N.; Belward, A.S. High-resolution mapping of global surface water and its long-term changes. *Nature* **2016**, *540*, 418–422. [[CrossRef](#)]
45. Brown, C.F.; Brumby, S.P.; Guzder-Williams, B.; Birch, T.; Hyde, S.B.; Mazzariello, J.; Czerwinski, W.; Pasquarella, V.J.; Haertel, R.; Ilyushchenko, S.; et al. Dynamic World, Near real-time global 10 m land use land cover mapping. *Sci. Data* **2022**, *9*, 251. [[CrossRef](#)]
46. Karra, K.; Kontgis, C.; Statman-Weil, Z.; Mazzariello, J.C.; Mathis, M.; Brumby, S.P. Global land use/land cover with Sentinel 2 and deep learning. In Proceedings of the 2021 IEEE International Geoscience and Remote Sensing Symposium IGARSS, Brussels, Belgium, 12–16 July 2021; IEEE: Piscataway, NJ, USA, 2021; pp. 4704–4707.

Disclaimer/Publisher’s Note: The statements, opinions and data contained in all publications are solely those of the individual author(s) and contributor(s) and not of MDPI and/or the editor(s). MDPI and/or the editor(s) disclaim responsibility for any injury to people or property resulting from any ideas, methods, instructions or products referred to in the content.